

Corrosion Inhibition of Carbon Steel by Anthraquinones Derivatives in 1.0 M HCl: Electrochemical and Quantum Calculations

L. Saqalli¹, M. Galai^{2,*}, N. Gharda¹, M. Sahrane¹, R. Ghailane¹, M. Ebn Touhami²,
Y. Peres-lucchese³, A. Souizi¹, N. Habbadi¹.

¹ Laboratory of Organic, Organometallic and Theoretical chemistry, Faculty of Science, Ibn Tofail University, PB 13314 000, Kénitra, Morocco.

² Laboratory of Materials Engineering and Environment: Modeling and Application, Faculty of Science, University Ibn Tofail BP. 133-14000, Kenitra, Morocco.

³ Laboratory of Chemical Engineering (Labège), BP 84234 Campus INP-ENSIACET, 4 allée Emile Monso, 31432 Toulouse Cedex 4, France

*E-mail: galaimouhsine@gmail.com

Received: 23 November 2017 / Accepted: 8 February 2018 / Published: 10 April 2018

The effect of hydroxyl group number of some anthraquinone derivatives 1,2,4-trihydroxyanthraquinone (purpurin) and 1,4-dihydroxyanthraquinone (quinizarin) on their corrosion inhibition efficiency has been reported in order to establish a relationship between inhibitor efficiency and molecular structure. Experimental study is based on the potentiodynamic polarization curves and electrochemical impedance spectroscopy (EIS). On the other hand, the quantum chemistry calculations were performed using B3LYP/6-31G (d) method to determine the electronic and structural parameters of the studied anthraquinone derivatives. The results revealed that the compound containing supplementary group (OH) presents the highest inhibition efficiency (91.5 %) in the case of Purpurin, that value is less than that obtained for Quinizarin (89.0 %). The experimental study indicated that the inhibition efficiency depends on concentration and molecular structure of the investigated compounds. The obtained experimental and theoretical results agree well and confirm that Purpurin, possessing the most number of OH group, is the better inhibitor.

Keywords 1,2,4-trihydroxyanthraquinone, 1,4-dihydroxyanthraquinone, Corrosion inhibitor, EIS, Polarization curves, DFT

1. INTRODUCTION

Corrosion is a phenomenon of degradation of metallic materials by the environment [1,2]. Corrosion causes waste of raw materials and energy and environmental damage and possibly costly in terms of human health [3,4]. This phenomenon concerns most industrial sectors, notably the automotive industry and the chemical and petrochemical industries [5, 6].

HCl solution is one of the most-used in many processes in the industrial sector; this acid causes the metallic degradation, due to its aggressiveness either by chemical or electrochemical reactions [7,8]

The use of inhibitors is one of the most practical methods [9, 10]. Inhibitors, which decrease corrosion on metallic materials, can be divided into three kinds: surfactant inhibitors [11], organic inhibitors [12] and inorganic inhibitors [13].

Several works have studied the influence of organic compounds on the corrosion of steel in acidic media [14-21]. Earlier reports [22-24] have been shown that inhibition efficiency of organic compounds containing hetero atoms and aromatic cycles is influenced by the nature and surface charge of metal by the electronic and chemical structure of inhibitor. However Additional to specific interactions between functional groups and metal surface, the group number can be influence the corrosion inhibition efficiencies.

Many research works have been developed in order to correlate group number and the inhibition efficiency of organic molecules [25,26].

The aim of this work is to explore the relationships between the anthraquinons derivative (1,2,4- trihydroxyanthraquinone and 1,4-dihydroxyanthraquinone) reactivity and their ability to inhibit the corrosion of carbon steel in in HCl solution to understand if any structural differences induced by different number of the hydroxyl group may be related to the experimentally observed differences of corrosion efficiency, using electrochemical measurements, also the kinetic and thermodynamic parameters are calculated and discussed . On the other hand, the quantum chemical calculations were determined using density functional theory (DFT) method to determine the global reactivity indices of the used inhibitors.

2. MATERIALS AND METHODS

2.1. Materials

The chemical composition of the carbon steel used is listed in Table 1.

Table 1. the composition of carbon steel

Elements	C	Si	Mn	Cr	Mo	Ni	Al	Cu	Co	V	W	Fe
(%) of Mass	0.11	0.24	0.47	0.12	0.02	0.1	0.03	0.14	<0.0012	<0.003	0.06	Balance

2.2. Inhibitors

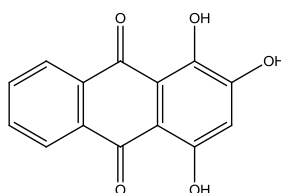


Figure 1. Chemical structure of Purpurin

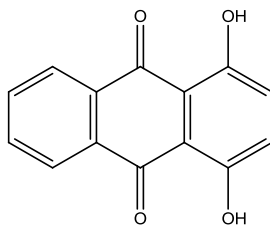


Figure 2. Chemical structure of Quinizarin

2.3. Solution

The tested solution was 1 M HCl which prepared by dilution of the commercial concentrated solution

2.4. Electrochemical method

Electrochemical experiments were performed by using three electrode with carbon steel (1 cm^2) as working electrode (WE), pt as an counter electrode and concerning the reference electrode (RE) we used the saturated calomel electrode S.C.E.

The potentiodynamic polarization curves were recorded by changing the electrode potential automatically from negative values to positive values versus E_{corr} using a Potentiostat/Galvanostat type PGZ 100, at a scan rate of 1 mV/s after 0.5 h of immersion time until reaching steady state.

The EIS experiments were conducted in the frequency range with high limit of 100 KHz and different low limit 100 mHz at open circuit potential, with 10 points per decade, at the rest potential, after 30 min of acid immersion, by applying 10 mV ac voltage peak-to-peak. Nyquist plots were made from these experiments

2.5. Computational method

For the theoretical study, the geometrical structure of Purpurin and Quinizarin were realized by using the Density Functional Theory (DFT) with the Beck's three parameter exchange functional and the Lee–Yang–Parr non-local correlation functional (B3LYP) [27,28] with 6-31G(d) basis set of atomic orbital as implemented in Gaussian 03 program package [29]. Furthermore, DFT method is proved as a very useful technique to probe the inhibitor/surface interaction as well as to analyze the experimental data [30].

It is well known that any physical or chemical property measured in a solvent can be different if it is measured in another solvent [31,32]. It is also expected that the inhibiting molecules in solution behave differently from those in vacuum. So, it is necessary to study the solvent effect on the geometrical structure and on the electronic properties, in order to take into account of this effect the polarized continuum model (PCM) [33] and water as solvent were used. In this model, the solvent was

treated as a continuum dielectric media and the solute is considered as a trapped molecule in a cavity surrounded by solvent.

The geometry structure was optimized under no symmetry constraint in gas and aqueous phases. The stability of the optimized geometry of the molecular structure was confirmed by harmonic vibration wave numbers calculated using analytic second derivatives which have shown the absence of imaginary frequency modes. The following quantum chemical parameters obtained from this optimized structure have been determined.

The energy of the highest occupied molecular orbital (EHOMO), is directly related to the ionization potential (I) and the energy of the lowest unoccupied molecular orbital (ELUMO) is directly related to the electron affinity (A), as follows:

$$A = -E_{LUMO} \quad (1)$$

$$I = -E_{HOMO} \quad (2)$$

The gap energy, is the difference in energy between the HOMO and LUMO,

The energetic gap is determined as follow:

$$\Delta E = E_{LUMO} - E_{HOMO} \quad (3)$$

The electronegativity (χ), the chemical potential (μ) and the global hardness (η) were evaluated, based on the finite difference approximation, as linear combinations of the calculated I and A:

$$\chi = -\mu = \frac{I + A}{2} \quad (4)$$

$$\eta = \frac{I - A}{2} \quad (5)$$

The fraction of transferred electrons (ΔN), evaluating the electronic flow in a reaction of two systems with different electronegativities in particular case a metallic surface and an inhibitor molecules, was calculated according to Pearson theory [34] as follows:

$$\Delta N = \frac{\chi_{Fe} - \chi_{inh}}{2(\eta_{Fe} + \eta_{inh})} \quad (6)$$

Where the indices Fe and inh refer to iron atom and inhibitor molecule, respectively

3. RESULTS AND DISCUSSION

3.1. Electrochemical study

the inhibition study of carbon steel corrosion in 1M HCl by Purpurin and Quinizarin was realized by using different electrochemical methods such as potentiodynamic polarization curves and electrochemical impedance spectroscopy (EIS).

3.2. Potentiodynamic Polarization curves

the potentiodynamic polarization curves of carbon steel in 1 M HCl in absence and presence of different concentrations of Purpurin and Quinizarin at 298K was presented in figure 3.

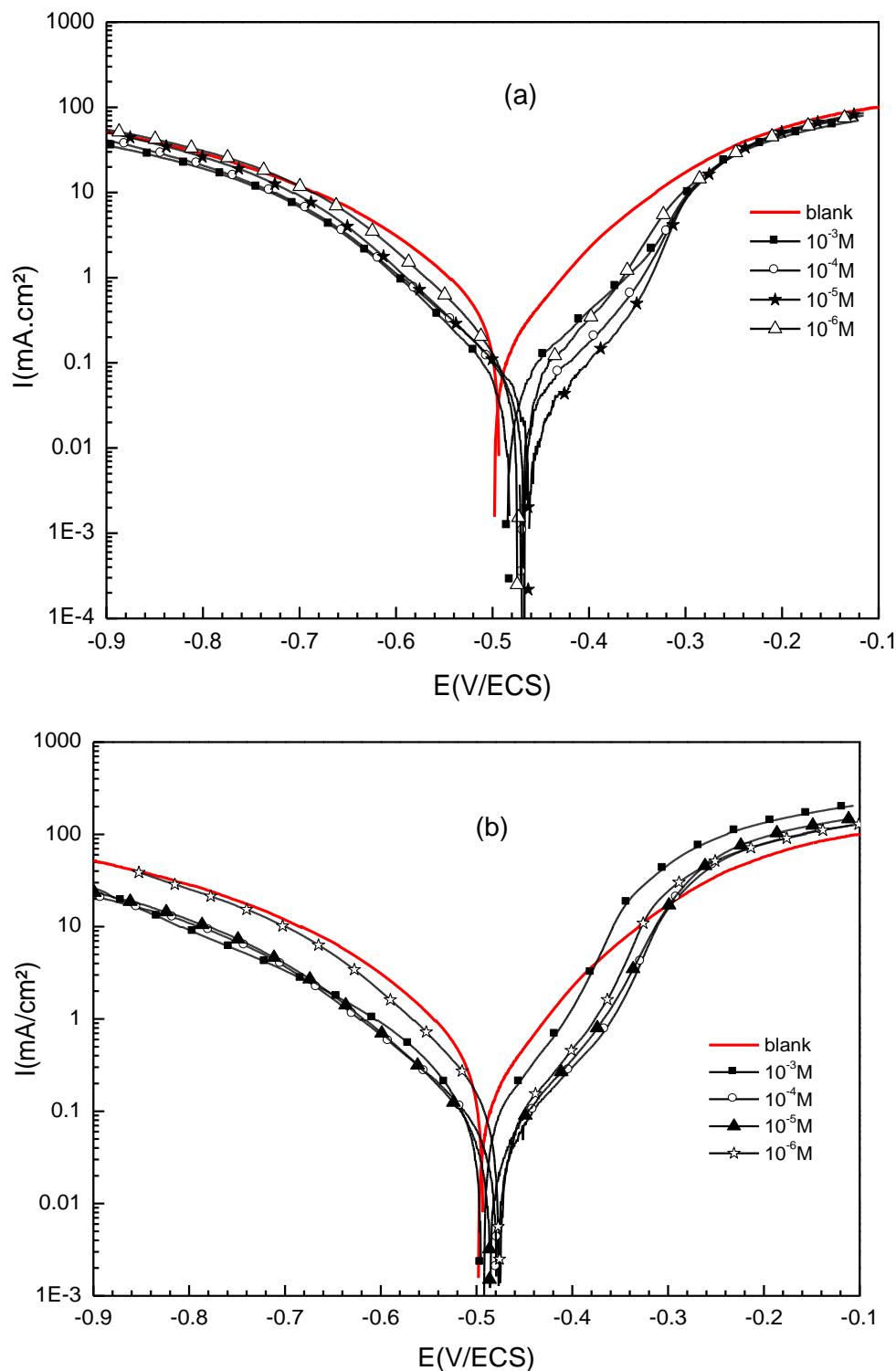


Figure 3. Potentiodynamic polarization curves of carbon steel in 1 M HCl without and with different concentrations of :(a) Purpurin (b) Quinizarin at 298K

Table 2. The electrochemical parameters obtained from polarization curves of carbon steel in 1 M HCl at various concentrations of two inhibitors

Inhibitor	Concentration(M)	$-E_{\text{corr}}$ (mV/SCE)	$-\beta_c$ (mVdec ⁻¹)	i_{corr} ($\mu\text{A}\cdot\text{cm}^{-2}$)	EI (%)
Blank	1.0	506.0	92	983.0	-----
Purpurin	10^{-6}	473.7	91	201	79.0
	10^{-5}	461.4	95	84	91.5
	10^{-4}	480.7	86	100	90.0
	10^{-3}	467.0	103	120	88.0
Quinizarin	10^{-6}	472.0	105	240	76.0
	10^{-5}	484.0	100	109	89.0
	10^{-4}	478.0	114	115	88.0
	10^{-3}	494.0	119	184	81.0

Fig. 3 (a, b) shows that the presence of the two inhibitors into the acid solution affects both region (anodic and cathodic), the anodic region was explained by the metal dissolution and the cathodic region by the hydrogen evolution reaction, the corrosion potential (E_{corr}) is slightly shifted. This implies that Purpurin and Quinizarin can be seen as a mixed-type inhibitors.

The electrochemical kinetic parameters, corrosion potential (E_{corr}), corrosion current density (I_{corr}), Tafel slopes (β_c) and inhibition efficiency, extract from the above plots are given in Table 2.

The inhibition efficiency, EI (%) was calculate by using the following equation [35]:

$$EI (\%) = \frac{i_{\text{corr}} - i_{\text{corr(inh)}}}{I_{\text{corr}}} \times 100 \quad (7)$$

Where i_{corr} and $i_{\text{corr(inh)}}$ are the corrosion current densities of uninhibited and inhibited solution respectively.

In the literature [36-40], an inhibitor can be classified as a cathodic or anodic type if the displacement in corrosion potential is more than 85 mV with respect to the corrosion potential of the blank. From the table 2, the corrosion potential of carbon steel shifted from 25.3 to 44.6 mV anodically compared to the blank in the case of Purpurin and from 12 to 34 in the case of Quinizarin, consequently, our inhibitors can be classified as a mixed type with the predominant anodic effectiveness of both inhibitors. This result is in good agreement with previous works for other inhibitors (table 3). The mixed-inhibition mechanism suggested by the polarization data is consistent with Shuduan [41], of E.E. Oguzie [42], and of H. Zarrok [43] on the adsorption behavior of organic molecules containing oxygen atom in acid solutions. Organic inhibitors may interact with the corroding metal and hence affect the corrosion reaction in more than one way, The adsorption mechanism for a given inhibitor depend on the functional groups present in its molecule, since different groups are adsorbed to different extents. Again, the presence of more than one functional group has been reported to often lead to changes in the electron density of a molecule, which could influence its adsorption behavior [44]

Table 3: Comparison between our studied inhibitors with other works that studied the mechanism of inhibition in the presence of organic inhibitors

Inhibitor	$-E_{\text{corr}}$ (mV/SCE)	$-\beta_c$ (mVdec ⁻¹)	i_{corr} ($\mu\text{A}\cdot\text{cm}^{-2}$)	EI (%)
Purpurin	461.4	95	84	91.5
Quinizarin	484	100	109	89.0
Methionine [42]	495	190	87	70.4
Alizarin violet 3B [41]	473	117	20	95.4
5-(2-chlorobenzyl) 2,6dimethylpyridazin-3-one [43]	469.8	199.4	48.8	95.5

The results show that when these inhibitors were added to 1HCl solution don't change the cathodic tafel, this may be indicate that Purpurin and Quinizarin adsorb onto the metal surface and minimize the corrosion rate by blocking the active sites of carbon steel surface.

The corrosion current density (i_{corr}) values decrease in the presence of these inhibitors. This indicates that these compounds' inhibit the corrosion process of carbon steel, by adsorption on the electrode surface. This adsorption of inhibitors on carbon steel surface non-bonding electron pairs present on aromatic rings and oxygen atoms as well as π -electrons [45]. This decrease is very pronounced in the case of Purpurin than in Quinizarin which can be attached to the slight difference between the two studied inhibitor molecules. This finding was confirmed by study at other authors [22,46-48] all of whom suggested that the effectiveness of an inhibitor is related to molecular structure; Danaee, Showed the effect of hydroxyl group position on adsorption behavior and corrosion inhibition, and definite the correlation of inhibition effect and molecular structure.

The efficiency values of inhibition increase with the decrease of the inhibitors concentration and reached the maximum value at 10^{-5} M indicating that the upper cover of the inhibitor on the surface of carbon steel is obtained in a solution with a lower concentration of inhibitors. The same results are obtained for other reports [49].

For Purpurin the maximum value is 91.5% and for Quinizarin is 89%. The results are clearly illustrating the fact that Purpurin presents the better inhibition than Quinizarin. Indeed, the present of OH supplementary group in the case of purpurin arises an enhancement in the inhibition efficiency. However, the high inhibitive performance of purpurin suggests a higher bonding ability on carbon steel surface, which possess a higher number of lone pairs on heteroatoms and π -orbitals, which are regarded as active adsorption centers. The electron lone pair on the oxygen atoms of the additional oxygen atoms will coordinate with the metal atoms of active sites caused a strong interaction with metal surface [50].

3.3. Electrochemical impedance spectroscopy

Figures 4a and 4b show impedance diagrams for carbon steel in acidic medium (1.0 M HCl) in the absence and the presence of various concentrations of Purpurin and Quinizarin. The results obtained are represented as diagrams of Nyquist [51].

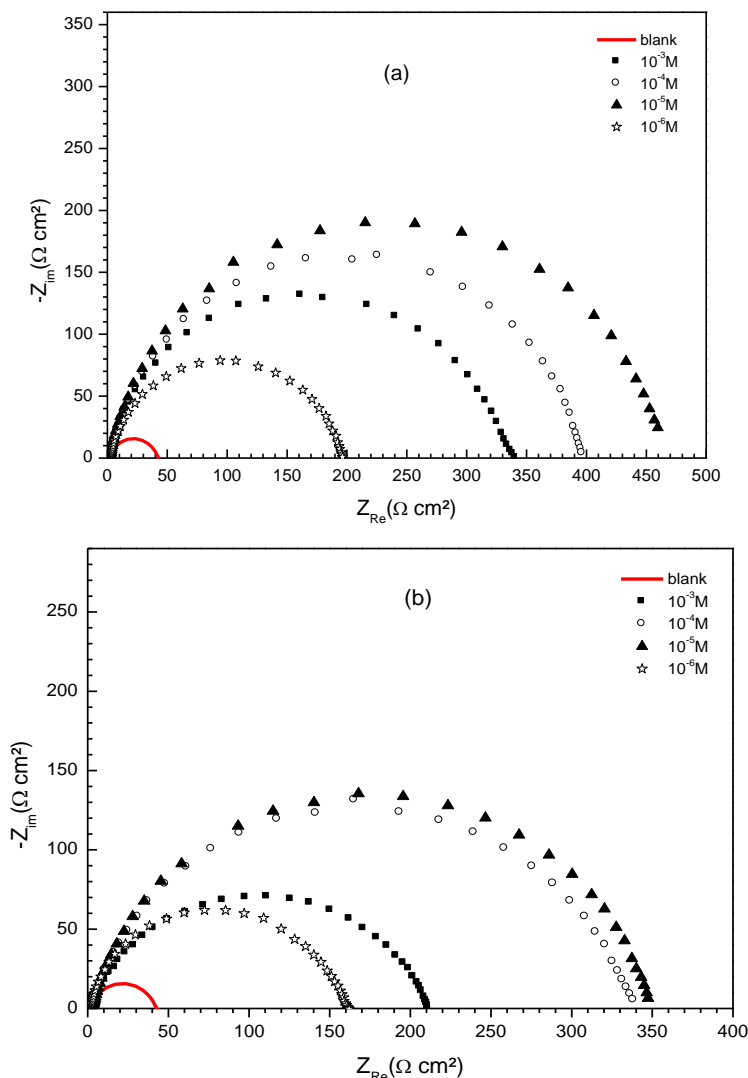


Figure 4. Nyquist plots for carbon steel in 1 M HCl without and with different concentrations of (a) Purpurin (b) Quiniarin.

It can be seen that the Nyquist plots were constituted of one semicircle which the diameter is related to the concentration and the type of the studied inhibitors.

The capacitive loop at high-frequency is related to the charge-transfer resistance (R_{CT}) and the double-layer capacitance (C_{dl}) [52, 53].

In both figures, the diameter of the capacitive loop is larger in the presence of inhibitor compared with blank solution. This process indicates that the impedance diagram of carbon steel in uninhibited acid solution increases after the addition of the Purpurin and Quiniarin as inhibitors in the aggressive solution. This indicates that the impedance of inhibited solution increases after the addition of purpurin and quiniarin inhibitors in blank solution.

In both diagrams the obtained Nyquist impedance is not perfect semicircles, this behavior can be attributed to the frequency dispersion effect as a result of the inhomogeneous of metal surface [54].

The equivalent circuit model employed to simulate the experimental data is mentioned in figure 5. In this equivalent circuit, R_s is the solution resistance, R_{ct} presents the charge transfer

resistance, and the CPE is the constant phase element which is used in place of double layer capacitance (C_{dl}) to give non-ideal capacitive behavior [55,56].

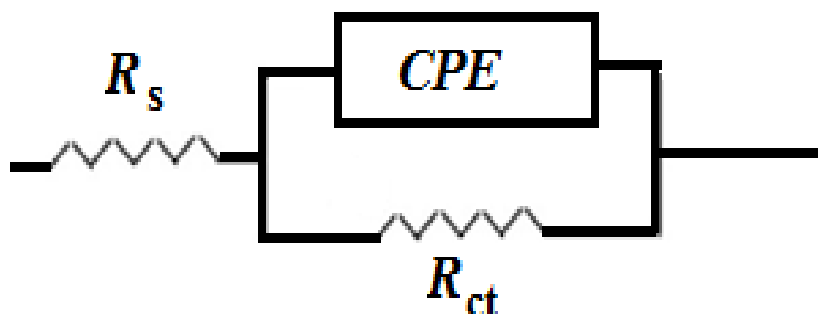


Figure 5. The equivalent circuit model used to fit the impedance diagrams.

Table 4. Electrochemical parameters for carbon steel in 1 M HCl at various inhibitors concentrations.

Inhibitor	Concentration (M)	R_{ct} (Ohm.cm ²)	C_{dl} (μF/cm ²)	η_z (%)
Blank	1.0	40.0	294	-----
Purpurin	10^{-6}	198	203	80.0
	10^{-5}	468	164	91.4
	10^{-4}	401	170	90.0
	10^{-3}	344.0	198	88.5
	Quinizarin	10^{-6}	161	214
	10^{-5}	348	111	88.5
	10^{-4}	340	144	88.0
	10^{-3}	201	192	80.0

The impedance parameters obtained from these plots are listed in Table 4. The charge transfer resistances (R_{ct}) are calculated from the difference between the values of impedance at low and high frequencies. The capacitance values (C_{dl}) is determined using the following equation [57]:

$$|C_{dl} = \frac{1}{2\pi f_{max} R_{ct}}$$

8

Where f_{max} represents the frequency at which imaginary value reaches a maximum on the Nyquist plot.

The inhibition efficiency (η_z %) was calculated by using the following formula [58] :

$$\eta_z \% = \frac{R_{ctcorr}^{-1} - R_{ctcorr(inh)}^{-1}}{R_{ctcorr}^{-1}} \times 100 \tag{9}$$

Where R_{ctcorr} and $R_{ctcorr(inh)}$ are the charge transfer resistance in the absence and presence of inhibitors, respectively.

It can be seen that the presence of the both inhibitors, the values of resistance charge transfer R_{ct} increase and the C_{dl} values reduce. Indicating that these inhibitors adsorb at the metal surface [59, 60]. Furthermore, the decreased values of C_{dl} may be due to a reduction in local dielectric constant and/or by an increase in the thickness of the electrical double layer [61].

Thus, the decrease of C_{dl} values, the increase in R_{CT} values and consequently the change of inhibition efficiency may be due to the gradual replacement of the water molecules by the adsorption of the Purpurin and Quinizarin molecules on the carbon steel surface, decreasing the extent of dissolution reaction. This result is in good accord with previous works [62,63]. For both cases, the efficiency values of inhibition increase substantially with the decrease of the concentration of the inhibitor, but the optimum value is 10^{-5} M indicating that the upper cover of the inhibitor on the surface is obtained in a solution with a lower concentration of inhibitors. The comparative study shows that Purpurin is more effective than Quinizarin and the difference in inhibitive efficiency mainly related to the structural differences between the Purpurin and Quinizarin induced by a different number of the hydroxyl group.

3.4. Effect of temperature

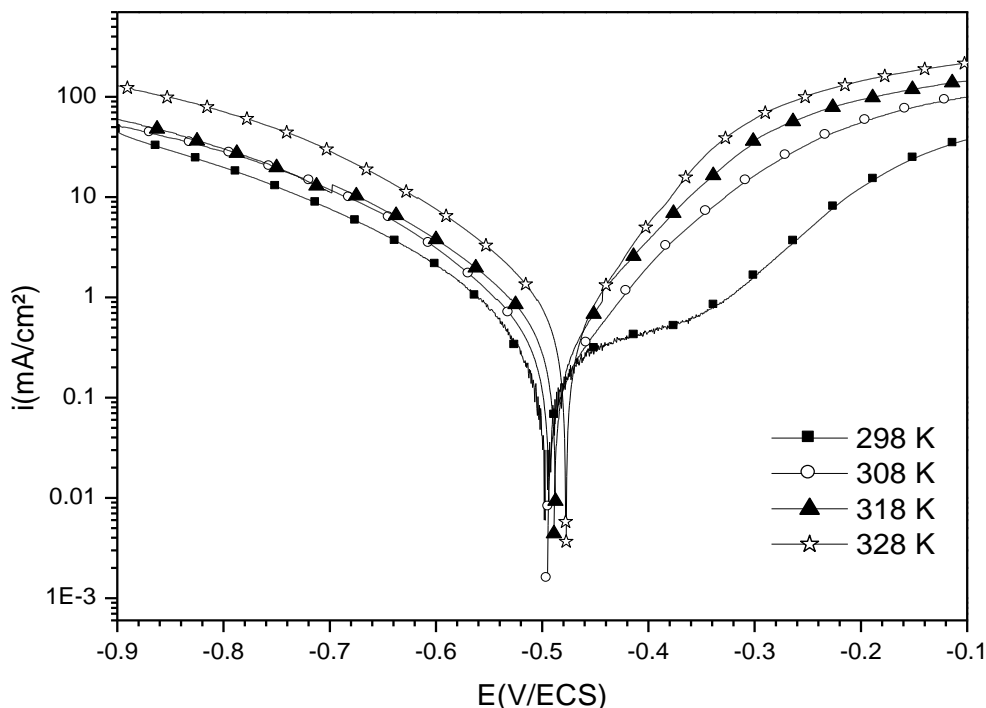


Figure 6. Polarization curves for carbon steel in 1M HCl at different temperatures.

The effect of temperature on the inhibition process in acidic solution has attracted the interest of a large number of researchers [64-66, 4] because the temperature can change the interaction between metal surface and the acidic medium in the absence and the presence of these inhibitor.

Therefore, we proposed to study this effect in order to explain the mechanism of adsorption and activation processes.

the potentiodynamic polarization were used to evaluate the effect of temperature on the corrosion processes of carbon steel surface in acidic media in the absence and presence of Purpurin and Quinizarin with the range of temperature 298, 308, 318 and 328 K (Figure 6 and 8) and the corresponding data are given in Table 5 and 6.

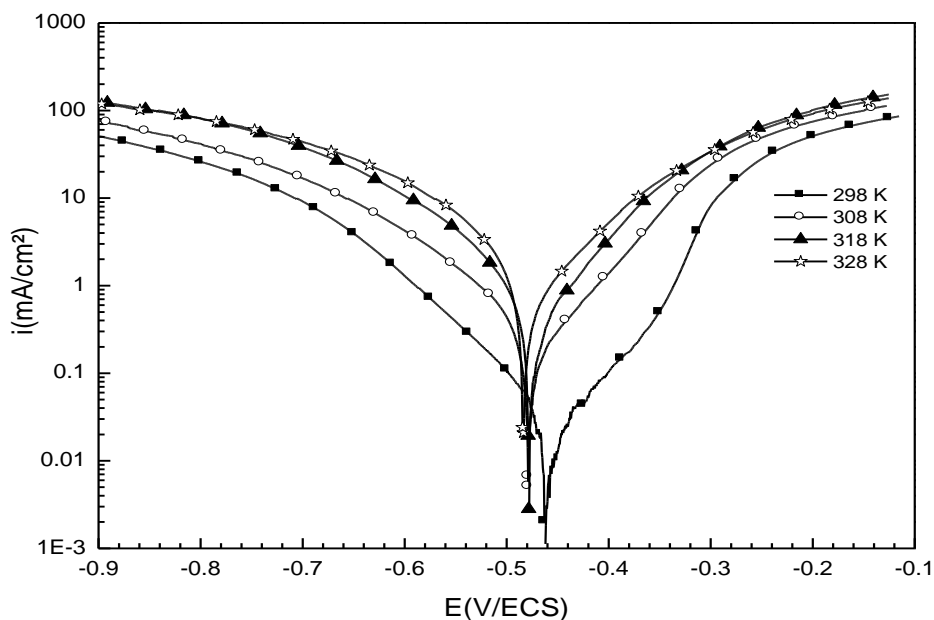


Figure 7. Polarization curves for carbon steel in 1 M HCl in the presence of Purpurin (10^{-5} M) at different temperatures.

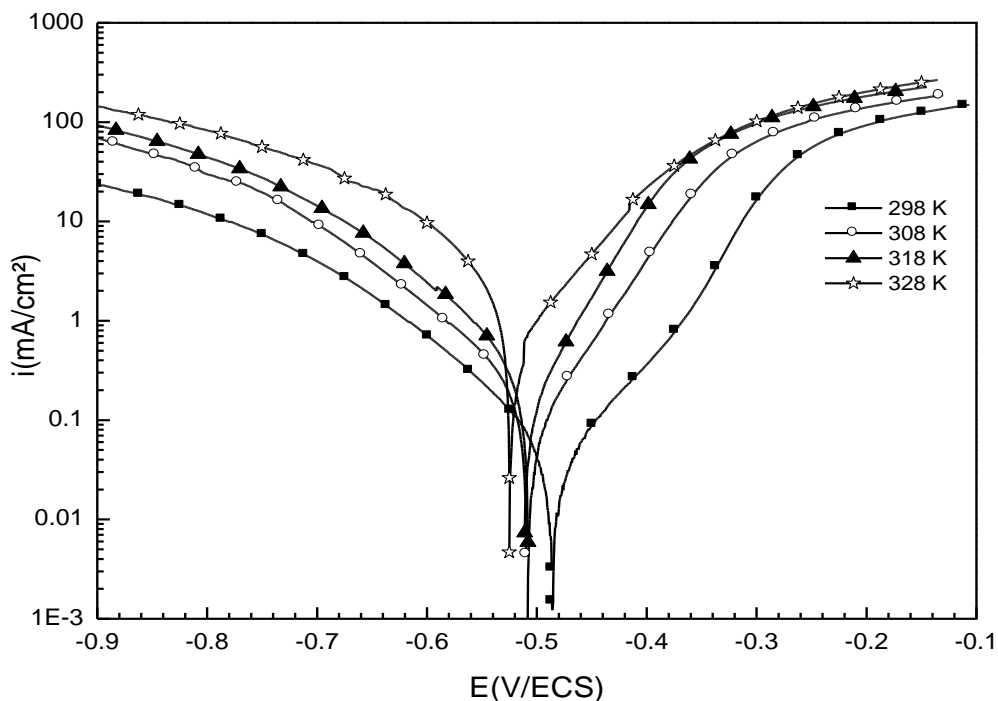


Figure 8. Polarization curves for carbon steel in 1.0 M HCl in the presence of quinizarin (10^{-5} M) at different temperatures.

Table 5. Electrochemical parameters for carbon steel in 1M HCl at different temperature

	E_{corr}(mV/ECS)	i_{corr}(μA/cm²)	β_c mV
25C°	-498	983	-92
35 C°	-491	1200	-184
45 C°	-475	1450	-171
55 C°	-465	2200	-161

Table 6. Electrochemical parameters for carbon steel in 1M HCl in presence of 10⁻⁵M of Quinizarin and Purpurin at different temperature

Inhibitor	Temperature (K)	-E _{corr} (mV/SCE)	-β _c (mV dec ⁻¹)	i _{corr} (μA cm ⁻²)	η (%)
Purpurin	298	461	95	84	91.5
	308	477	101	144	88
	318	477	105	205	86
	328	483	90	320	85
Quinizarin	298	484	100	109	89
	308	508.3	111.6	220	82
	318	506.9	89.6	278	81
	328	524.0	108.7	481	78

from Table 6 it is clear that the corrosion current density i_{corr} increases with increasing temperature but the temperature has not changed the significantly inhibitory performance of Purpurin and Quinizarin. Indeed its efficiency inhibitory are nearly constant, recorded a slight decrease when the temperature varies from 298 K (91.5 %) to 328 K (85 %) for Purpurin and 89 % to 78 % for Quinizarin.

The noticeable decrease of the inhibitor efficiency (85 %) for Purpurin and (78%) for Quinizarin is observed at the temperature (328 K), this decrease may be demonstrated by desorption of the both inhibitors Purpurin similar to Quinizarin from the electrode surface. The obtained results are in accord with previous investigations [67, 68].

3.5. Thermodynamic parameters

To strengthen the process of corrosion, the activation parameters like Enthalpy (ΔH°), Entropic (ΔS°) and the apparent activation Energie (E_a), are calculated and discussed.

The activation Energie (E_a) can be calculated by the Arrhenius equation [69]:

$$i_{\text{corr}} = k \exp\left(-\frac{E_a}{RT}\right) \quad (10)$$

Where T is the absolute temperature, i_{corr} is the corrosion current densities, k is the constant preexponential factor and R is the universal gas constant.

Arrhenius plots for the corrosion rate of carbon steel are given in Figure 9 are used to calculate the activation energy (E_a).

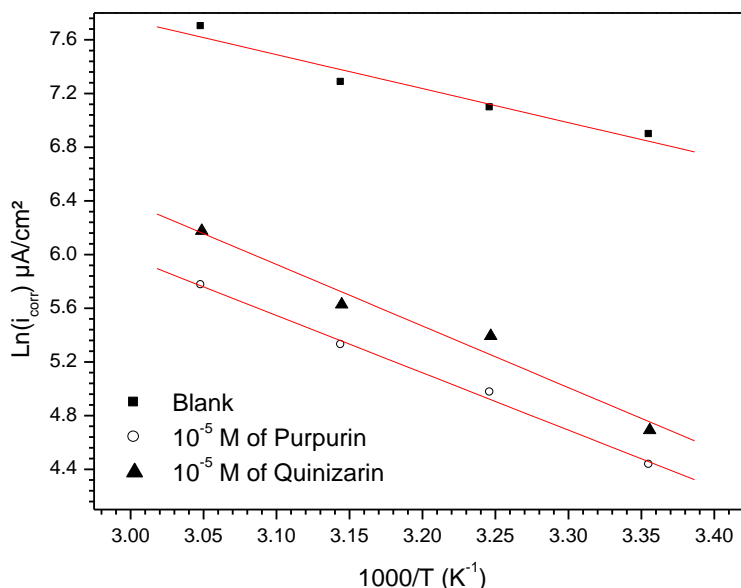


Figure 9. Arrhenius plots for carbon steel in 1 M HCl solution with and without of 10^{-5} M of Quinizarin and Purpurin

Table 7. The activation energy calculated in absence and in presence of Alizarin

Inhibitor	E_a (kJ mol ⁻¹)
Blank	21.0
Purpurin	35.5
Quinizarin	38.0

The E_a values obtained from these plots are given in the table. 7. analyze of these value shows that the energy of activation in the presence of inhibitors is higher than that in the absence.

The higher activation energy may be interpreted as physical adsorption at the metal surface indeed, a higher energy barrier for the corrosion process in the blank solution solution is associated with physical adsorption or weak chemical bonding between the inhibitors molecules and the carbon steel surface [70]. Similar results obtained for other inhibitor molecules have been reported elsewhere [71].

Other kinetic data like enthalpy (ΔH_a) and entropy of adsorption (ΔS_a) are accessible using the alternative formulation of Arrhenius equation [72]:

$$I_{\text{corr}} = \left(\frac{RT}{Nh}\right) \exp\left(\frac{\Delta S^\circ}{R}\right) \exp\left(\frac{-\Delta H^\circ}{RT}\right) \tag{11}$$

Where h is the Plank's constant and N is Avogadro's number, ΔH_a the enthalpy of activation and ΔS_a the entropy of activation.

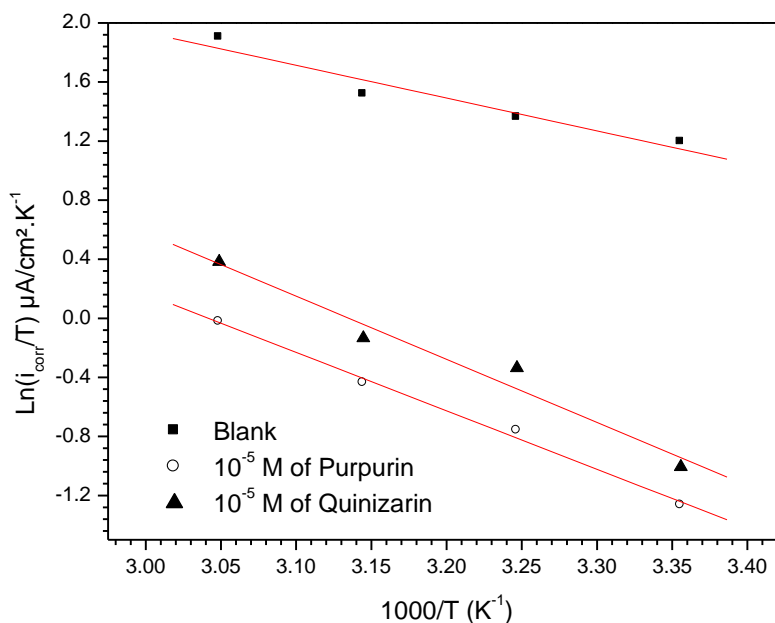


Figure 10. Variation of $\text{Ln}(i_{\text{corr}} / T)$ as function of the inverse of the temperature in the absence and the presence of 10^{-5} of Purpurin and Quinizarin

Figure 10 present the variation of $\ln\left(\frac{i_{\text{corr}}}{T}\right)$ function ($1/T$) as a straight line with as lope of $\Delta H_a / R$) and the intersection with then-axis is $[\text{Ln}(R/Nh) + (\Delta S_a / R)]$. From these plots, the values of ΔS_a and ΔH_a can be determined .The activation parameters such as ΔH_a and ΔS_a in the absence and presence of inhibitors are listed in table 8.

Table 8. the values of $\Delta H_{\text{abs}}^\circ$ and $\Delta S_{\text{ads}}^\circ$ for carbon steel in acidic medium in the absence and presence 10^{-5} M of Purpurin and Quinizarin (10^{-5}).

Inhibitor	$\Delta H_{\text{abs}}^\circ$ (KJ. mol ⁻¹)	$\Delta S_{\text{ads}}^\circ$ (J.mol ⁻¹ .K ⁻¹)
blank	18.4	-126
Purpurin (10^{-5} M)	32.8	-97.5
Quinizarin (10^{-5} M)	35.5	-86.1

According to A. Tazouti [73] the positive sign of the enthalpy reflects the endothermic nature; the negative signs of ΔH_a values reflect the exothermic nature of the carbon steel dissolution .

Here the calculated value of ΔH° for dissolution reaction of carbon steel in 1.0 M HCl in the presence of Purpurin and Quinizarin is higher than that in blank solution . The positive signs reflect the endothermic nature of the carbon steel dissolution process .

All values of E_a are higher than the values of ΔH_a , this observation indicate that the corrosion process controlled by gaseous reaction, simply the hydrogen evolution reaction, associated with a decrease in the total reaction volume [74].

The ΔS° values are negative in the tow case (the uninhibited and inhibited solutions). The increase of ΔS° value indicates an increase of the disorder this can be generally interpreted by the conversion of the reactants to the activated complexes which take place at the interface metallic surface/solution [75].

3.6. Adsorption isotherms

Adsorption isotherms are very important in understanding the mechanism of organo-electrochemical reactions[76]. In order to evaluate the adsorption process of LO onto carbon steel surface, Langmuir adsorption isotherm were obtained according to the following equations:

$$\frac{C_{inh}}{\theta} = \frac{1}{K_{ads}} + C_{inh} \quad (\text{Langmuir}) \quad (12)$$

Where θ is the surface coverage of the metal surface, K the adsorption-desorption equilibrium constant, C_{inh} the inhibitor concentration and a is the lateral interaction term describing the molecular interactions in the adsorption layer and the surface heterogeneity. The fractional coverage values θ as a function of inhibitor concentration can be obtained from polarization curve as follows:

$$\theta = \frac{i_{corr} - i_{corr/inh}}{i_{corr}} \quad (13)$$

The data were tested graphically, see figure 11 by fitting to Langmuir isotherm which given by equations 6.

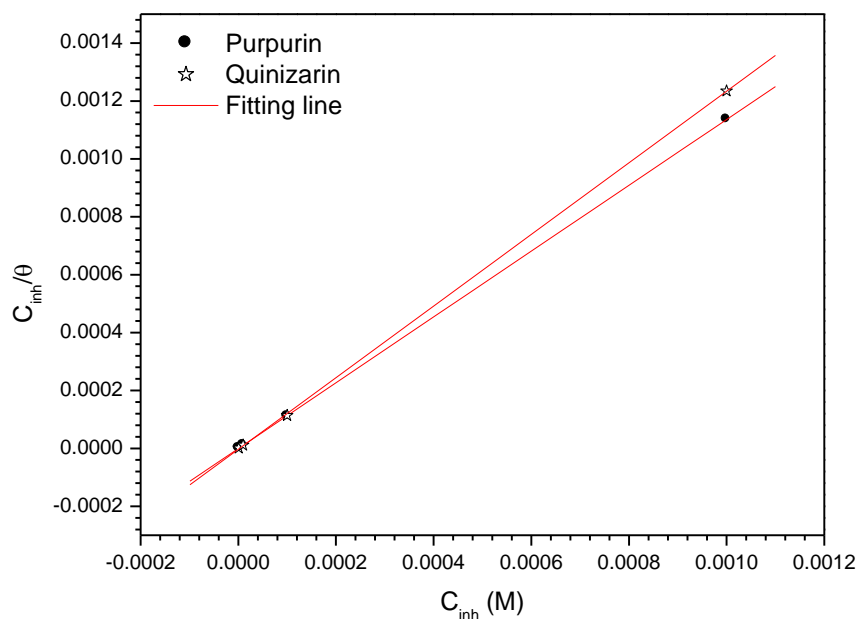


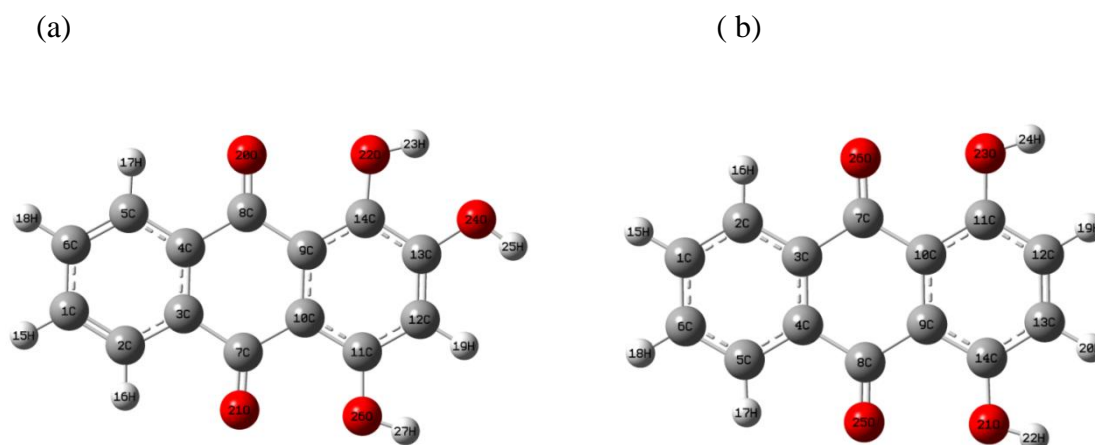
Figure 11. Langmuir adsorption plots obtained for carbon steel in 1 M HCl containing different concentrations of Purpurin and Quinizarin at 298 K.

Table 9. Adsorption parameters from Langmuir Kinetic isotherms for carbon steel in 1M HCl in the absence and presence of Purpurin and Quinizarin at 298 K.

Inhibitors	Langmuir		
	K_{ads} (M^{-1})	ΔG_{ads} (kJ/mol)	R^2
Purpurin	1.1×10^8	55.8	1
Quinizarin	2.8×10^7	41	0.99997

The analysis of figure 11 shows that the variation of the ratio C_{inh} / θ as a function of the inhibitor concentration is linear for the Langmuir isotherm, indicating that the adsorption of Purpurin and Quinizarin on the surface of the steel in 1M HCl obeys the Langmuir adsorption isotherm. Consequently, the inhibition of the corrosion is due to the formation of layer on the metallic surface, limiting electrolyte access, the strong correlations ($R^2 = 0.995$) confirm the validity of this chosen model. Furthermore, it is recognized that the ΔG_{ads} values of less than or equal to 20 KJ/mol indicate that the adsorption mode is physical, whereas those with values greater than 40 KJ/mol involve sharing or transfer of electrons from the inhibitor compound to the metal surface to form a co-ordinate type of bond (chemisorption) according to several authors [77]. From the table 9, the values of the free enthalpy of adsorption ΔG_{ads} are greater than 40 KJ/mol for the two inhibitors. So, we can consider that these inhibitors are chemically adsorbed on the mild steel surface in 1.0 M of hydrochloric acid solution.

3.7. Quantum chemical calculation

**Figure 12.** Optimized molecular structure of (a) Purpurin and (b) Quinizarin.

The quantum chemical parameters were calculated by using density functional theory (DFT) method to correlate some quantum chemical parameters with experimental inhibition efficiencies of (a) Purpurin and (b) Quinizarin.

3.7. Molecular geometry

The molecule's structure was built with the Gauss View 3.0 implemented in Gaussian 03 package [78], their corresponding geometries were fully optimized at B3LYP/6-31G (d) level of theory.

Table 10. Some geometrical parameters of Purpurin are determined at B3LYP/6-31G (d) level of theory in gas (G) and in solvent (S).

		Bond length (Å)		Bond angle (°)		Bond angle (°)	
purp	G	C3-C7	1.493	C3-C7-C10	117.8	C3-C7-O21	119.5
	S		1.493		118.0		119.0
	G	C7-C10	1.489	C7-C10-C9	120.8	C10-C7-O21	122.7
	S		1.480		120.7		123.0
	G	C9-C10	1.433	C10-C9-C8	120.6	C9-C14-O22	123.1
	S		1.439		120.6		123.3
	G	C8-C9	1.496	C9-C8-C4	117.8	C13-C14-O22	118.0
	S		1.489		118.0		117.4
	G	C4-C8	1.491	C8-C4-C3	121.4	C12-C13-O24	124.1
	S		1.489		121.2		124.7
	G	C3-C4	1.402	C4-C3-C7	121.5	C14-C13-O24	114.5
	S		1.403		121.5		114.1
	G	C10-C11	1.410	C7-C10-C11	120.0	C10-C11-O26	120.6
	S		1.411		120.5		120.6
	G	C11-C12	1.405	C10-C11-C12	120.0	C12-C11-O26	119.4
	S		1.406		120.4		119.0
	G	C12-C13	1.380	C11-C12-C13	120.4		
	S		1.378		120.3		
	G	C13-C14	1.413	C12-C13-C14	121.4		
	S		1.419		121.2		
	G	C14-C9	1.403	C13-C14-C9	118.9		
	S		1.401		119.3		
	G	C7=O21	1.227	C14C9-C10	120.3		
	S		1.233		120.0		
	G	C8=O20	1.225	C9-C10-C11	119.1		
	S		1.231		118.9		
	G	C11-O26	1.358	C14-C9-C8	119.1		
	S		1.356		119.4		
	G	C13-O24	1.370	C4-C8-O20	119.9		
	S		1.359		119.6		
	G	C14-O22	1.354	C9-C8-O20	122.2		
	S		1.355		122.4		

From the Table 10, the bond length C-C vary between 1.402 Å and 1,496 Å for the bi-substituted ring by C=O group. For the aromatic cycle substituted by hydroxyl groups, the bond length values of C-C are lower (1.380-1.413 Å) than the previous ones. The bond length values of C=O and C-OH are (1.225-1.227 Å) and (1.354-1.370 Å) respectively.

For the substituted rings, the bond angle values of C-C-C vary between 117° and 122° which is closely comparable to 120°.

The solvent effect can be estimated by the determination of the difference between the geometrical parameters calculated in the gas and aqueous phases. For the inter-atomic distances, this difference for C-C bond is about 0.009 Å, whereas it is valued to 0.006 Å for C=O polarized bond. The highest effect is observed for C₁₃-O₂₄ whose bond length value decreases by about 0,011 Å in aqueous phase.

Table 11. Some geometrical parameters of Quinizarin calculated at B3LYP/6-31G (d) level of theory in gas (G) and in solvent (S).

	Bond length (Å)		Bond angle (°)		Bond angle (°)	
G	C3-C7	1.491	C3-C7-C10	118.0	C4-C8-O25	119.7
S		1.490		118.2		119.3
G	C7-C10	1.496	C7-C10-C9	120.7	C3-C7-O26	119.7
S		1.489		120.5		119.3
G	C9-C10	1.428	C10-C9-C8	120.7	C10-C7-O26	122.3
S		1.435		120.5		122.5
G	C8-C9	1.496	C9-C8-C4	118.0	C9-C14-O21	120.7
S		1.489		118.0		121.0
G	C4-C8	1.491	C8-C4-C3	121.4	C13-C14-	119.9
S		1.490		121.2	O21	119.4
G	C10-C11	1.412	C7-C10-C11	120.0	C10-C11-	120.7
S		1.411		120.0	O23	121.0
G	C11-C12	1.402	C10-C11-C12	119.4	C12-C11-	119.9
S		1.406		119.5	O23	119.4
G	C12-C13	1.381	C11-C12-C13	121.0		
S		1.377		121.0		
G	C13-C14	1.402	C12-C13-C14	121.0		
S		1.406		121.0		
G	C14-C9	1.412	C13-C14-C9	119.4		
S		1.411		120.0		
G	C7=O26	1.225	C14-C9-C10	119.6		
S		1.231		119.5		
G	C8=O25	1.225	C9-C10-C11	119.6		
S		1.231		119.5		
G	C11-O23	1.358	C14-C9-C8	119.7		
S		1.357		120.0		
G	C14-O21	1.358	C9-C8-O25	122.3		
S		1.357		122.5		

The results given in table 11 show that the bond length C-C vary between 1.428 Å and 1,496 Å for the bi-substituted ring by C=O group. For the aromatic cycle substituted by hydroxyl groups, the bond length values of C-C are lower (1.381-1.412) than the previous ones. The bond length values of C=O and C-OH are 1.225 and 1.358 respectively.

For the substituted rings, the bond angle values of C-C-C vary between 118° and 122° which agree well with the planarity of the molecule.

In presence of the solvent the bond lengths C-C undergo a variation which is about 0.007 Å, whereas the bond length C=O increase by 0.006 Å.

3.6. Global molecular reactivity

Table 12. The calculated electronic parameters of Purpurin and Quinizarin.

	Phase	E_{HOMO}	E_{LUMO}	$\Delta E(\text{eV})$	μ	PI	$A E$	χ	η	ΔN	%IE
purp	G	-5.842	-2.368	3.474	5.1174	5.842	2.368	4.105	1.737	0.833	91.5
	S	-5.928	-2.627	3.301	7.2426	5.928	2.627	4.277	1.651	0.825	
quini z	G	-6.074	-2.550	3.524	3.3206	6.074	2.550	4.312	1.762	0.763	89.0
	S	-6.111	-2.731	3.380	4.9739	6.111	2.731	4.421	1.690	0.763	

The highest occupied molecular orbital energy level (E_{HOMO}) is associated with the electron donating ability of a molecule, that can explain the adsorption taking place on the interface (metallic surface-inhibitory molecule) when the inhibitor possess delocalized electrons π . High values of E_{HOMO} are likely to indicate a tendency of the molecule to donate electrons to appropriate acceptor molecules with low empty molecular orbital energy. The energy of the lowest unoccupied molecular orbital (E_{LUMO}) which is related to electron affinity signifies the electron receiving tendency of a molecule. A low value of LUMO energy show more probability to accept electrons [79].

The energy gap between LUMO and HOMO is an important parameter in determining molecular electrical transport properties because it is a measure of electron conductivity. On the other hand, that is a function able to anticipate the reactivity of the inhibitor molecule in the adsorption process on the metallic surface. When the energy gap value ΔE decreases the reactivity of molecular system increases, the inhibitor efficiency is improved [80].

According to the results listed in Table 12, a smaller value of ΔE (3.474 eV) is found for Purpurin in comparison to quinizarin (3.524 eV). Therefore, higher inhibition efficiency indicates that the Purpurin is very reactive and can be easily adsorbed on the metallic surface, thus it can be considered as effective corrosion inhibitor. This conclusion is in good agreement with experimental results. In presence of the solvent the energy gap decreases by 0.173 eV for Purpurin, and 0.144 eV for Quinizarin, this lets us to conclude that reactivity increases in presence of water as solvent which promotes the electron transition and the charge transfer.

The dipolar moment provides information on the polarity of the whole molecule. High dipole moment values are reported to facilitate adsorption by influencing the transport process through the adsorbed layer [81]. From the table 12 the dipole moment (μ) of Purpurin in gas is (5.1174 D) which is higher than that of Quinizarin (3.3206 D), indicating that Purpurin molecule is strongly polarizable. Several authors have stated that the inhibition efficiency increases with dipole moments values [82,83]. In addition, it is noted that the value of the dipole moment in presence of polar solvent (H_2O) is $\mu=$

7.2426 D for Purpurin and 4.9739 D for Quinizrin indicating that the polarization increases by 2.1252 and 1.6533 D for Purpurin and Quinizarin respectively in presence of the solvent. To sum up, the reactivity of this molecule increases in aqueous solution.

The Calculated values of electronegativity (χ), the global hardness (η) are also presented in Table 12. It is well known that the inhibitor with the least value of hardness is the most reactive and vice versa, or in another way a soft molecule is more reactive than the hard one. As shown in Table 12, the values of η for Purpuin are slightly lower than those obtained for Quinizarin in the both phases, this explains that Purpurin is slightly more efficient against corrosion than Quinizarin.

The comparison between the values obtained for hardness and electronegativity in solvent shows a slight variation of these parameters, indeed the electronegativity increase and the hardness decrease in presence of solvent is due to the polarization, of the inhibitor molecule, involved by the presence of polar solvent H₂O.

The fraction of electrons transferred (ΔN) from inhibitor to carbon steel surface is another important factor. The ΔN values are correlated to the inhibition efficiency resulting from electron donation. The values of (ΔN) clearly revealed that the inhibition efficiency increased with the ΔN increase [84].

The fraction of electron transferred, was calculated using the Equation below:

$$\Delta N = \frac{\chi_{Fe} - \chi_{inh}}{2(\eta_{Fe} + \eta_{inh})} \quad 12$$

Where χ_{Fe} and χ_{inh} are the electronegativity of Fe and the inhibitor respectively, and can be evaluated as η_{Fe} and η_{inh} are the global hardness of Fe and the inhibitor respectively. The theoretical values of χ_{Fe} and η_{Fe} are 7 and 0 eVmol⁻¹ respectively [85].

According to Lukovits study [86], if $\Delta N < 3.6$, the inhibition efficiency increases with increasing electron- donating ability at the metal surface. The obtained values of ΔN reported in Table 10 shows that the inhibitors are the donators of electrons and the iron surface is the acceptor.

One of the most important parameter in the determination of efficiency of the inhibitor is the amount of electric charge exchanged between inhibitor and metallic surface when the adsorption process takes place. From the results giving in table 11, it is shown that the charge transferred ΔN (0.833) from Purpurin is slightly higher than that

calculated for Quinizarin (0.763) in vacuum this can explain that Purpurin is more efficient than Quinizarin this result is in good agreement with the experiment. Furthermore, it is noticeable that there isn't any solvent effect on the ΔN value of the Quinizarin, whereas a decrease of 0.008 is observed for Purpurin.

4. CONCLUSION

The effect of hydroxyl group number on the adsorption behavior and corrosion inhibition of anthraquinon derivatives has been studied on carbon steel electrode in 1 M HCl by using different electrochemical measurements and quantum calculations at B3LYP/6-31G(d) level of theory. From the experimental results mentioned above, it can be concluded that:

- The inhibition efficiency increased with the decrease of the concentration of the inhibitors to reach a maximum value at 10^{-5} M.
- The obtained results show the same trend from electrochemical impedance and the polarization measurements.
- Polarization measurements show that these inhibitors can be classified as a mixed type with anodic predominance.
- From the electronic parameters, it was found that inhibition efficiency increased when the values of ELUMO and energetic gap (HOMO-LUMO) decrease and when the values of dipolar moment and the fraction of transferred electrons increased.
- The inhibitor efficiency of anthraquinon derivatives depend on the number of the hydroxyl group contained in these molecules, indeed it has been deduced that the high inhibitor efficiency is observed for purpurin possessing the high number of OH group.

References

1. K. Mansouri, M. Saidi and M. Dakmouche, *J. Adv. Res. Sci. Technol.*, 2 (1) (2015) 130-138.
2. T. Fukuma, *Scientific Instruments News.*, 8 (2017).
3. M. Finšgar and J. Jackson, *Corros. Sci.*, 86 (2014) 17-41.
4. N. Gharda, M. Galai, L. Saqalli, M. Ouakki, N. Habbadi, R. Ghailane, A. Souizi, M. EbnTouhami and Y. Peres-lucchese, *Orient. J. Chem.*, 33 (4) (2017) 1665-1676.
5. F. Ropital, *mater. Corros.*, 60(2009) 495-500.
6. M. B. Kermani, and D. Harrop, *SPE Production & Facilities.*, 11(3) (1996) 186-190.
7. M. Gupta, J. Mishra and K.S.Pitre, *Int. J. Corros.*, 1 (2013) 1-5.
8. S.M. Shaban, A. Saied, S.M. Tawfik, A. Abd-Elaal and I. Aiad, *J. Ind. Eng. Chem.*, 19 (6) (2013) 2004-2009.
9. I.B.Obot, N.O. Obi-Egbedi and S.A.Umoren, *Corros. Sci.*, 51 (8) (2009) 1868-1875.
10. M. Lebrini, F. Robert, H. Vezin and C.Roos, *Corros. Sci.*, 52(10) (2010) 3367-3376.
11. A.M. Al-Sabagh, H.M. Abd-El-Bary, R.A. El-Ghazawy, M.R. Mishrif and B.M. Hussein, *Egyptian Journal of Petroleum.*, 21 (2) (2012) 89-100.
12. L. Lakhrissi, B. Lakhrissi, R. Tourir, M. E. Touhami, M. Massoui and E.M. Essassi, *Arabian J. Chem.*, 10 (2) (2017) S3142-S3149.
13. A. Ait Aghzzaf, B. Rhouta, E. Rocca and A. Khalil, J. Steinmetz. *Corros. Sci.*, 80 (2014) 46-52.
14. L. Saqalli, M. Galai, F. Benhiba, N. Gharda, N. Habbadi, R. Ghailane, M. Ebn Touhami, Y. Peres-lucchese, A. Souizi and R. Tourir, *J. Mater. Environ. Sci.*, 8 (2017) 2455-2467.
15. E. Oguzie, C. Akalezi and C. Enenebeaku, *Pigm. Res. Technol.*, 38 (2009) 359-365.
16. Y. Abboud, A. Abourriche, T. Saffaj, M. Berrada, M. Charrouf, A. Bennamara and H Hannache, *Desalination.*, 237 (2009)175-189.
17. E.E. Ebsenso, H. Alemu, S.A. Umoren and I.B. Obot, *Int. J. Electrochem. Sci.*, 3 (2008) 1325-1339.
18. A. Zarrouk, A. Dafali, B. Hammouti, H. Zarrok, S. Boukhris and M. Zertoubi, *Int. J. Electrochem. Sci.*, 5 (2010) 46.
19. M. Mihit, K. Laarej, H. Abou El Makarim, L. Bazzi, R. Salghi and B. Hammouti, *Arabian J. Chem.*, 3 (2010) 55.
20. A. Zarrouk , B. Hammouti, A. Dafali and H. Zarrok, *Der Pharma Chemica.*, 3 (4) (2011) 266.
21. A. Zarrouk, B. Hammouti, H. Zarrok, M. Bouachrine, K.F. Khaled and S.S. Al-Deyab, *Int. J. Electrochem., Sci.*, 6 (2012) 89.
22. I. Danaee, O. Ghasemi, G.R. Rashed, M. R. Avei and M. H. Maddahy, *J. Mol. Struct.*, 1035 (2013)

- 247-259.
23. Z. El. Adnani, M. Mcharfi, M. Sfaira, M. Benzakour, A.T. Benjelloun and M. Ebn Touhami, *Corros. Sci.*, 68 (2013) 223–230.
 24. P. Mohan and G.P. Kalaignan, *J. Mater. Sci. Technol.*, 29 (2013) 1096–1100.
 25. Understanding the corrosion inhibition of carbon steel and copper in sulphuric acid medium by amino acids using electrochemical techniques allied to molecular
 26. K. F. Khaled, K. Babić-Samardžija and N. Hackerman, *Electrochimica. Acta*, 50 (12) (2005) 2515-2520.
 27. C. Lee, W. Yang and R.G. Parr, *Phys. Rev. B.*, 137 (1988) 785-789
 28. A.D. Becke, *J. Chem. Phys.*, 98 (1993) 1372-1377.
 29. M. J. Frisch, G. W. Trucks, H. B. Schlegel, G. E. Scuseria, M.A. Robb, J. R. Cheeseman, J. A. Jr. Montgomery, T. Vreven, K. N. Kudin, J. C. Burant, J. M. Millam, S. S. Iyengar, J. Tomasi, V. Barone, B. Mennucci, M. Cossi, G. Scalmani, N. Rega, G.A. Petersson, H. Nakatsuji, M. Hada, M. Ehara, K. Toyota, R. Fukuda, J. Hasegawa, M. Ishida, T. Nakajima, Y. Honda, O. Kitao, H. Nakai, M. Klene, X. Li, J. E. Knox, H.P. Hratchian, J. B. Cross, C. Adamo, J. Jaramillo, R. Gomperts, R. E. Stratmann, O. Yazyev, A. J. Austin, R. Cammi, C. Pomelli, J.W. Ochterski, P.Y. Ayala, K. Morokuma, G. A. Voth, P. Salvador, J. J. Dannenberg, V. G. Zakrzewski, S. Dapprich, A. D. Daniels, M. C. Strain, O. Farkas, D. K. Malick, A.D. Rabuck, K. Raghavachari, J. B. Foresman, J. V. Ortiz, Q. Cui, A. G. Baboul, S. Clifford, J. Cioslowski, B. B. Stefanov, G. Liu, A. Liashenko, P. Piskorz, I. Komaromi, R. L. Martin, D. J. Fox, T. Keith, M. A. Al-Laham, C. Y. Peng, A. Nanayakkara, M. Challacombe, P. M. W. Gill, B. Johnson, W. Chen, M. W. Wong, C. Gonzalez and J. A. Pople, *Gaussian 03, Revision B. Pittsburgh, PA, USA: Gaussian, Inc.*, (2003).
 30. N.O. Obi-Egbedi, I.B. Obot and M.I. El-Khaiary, *J. Mol. Struct.*, 1002 (2011) 86-96
 31. M.A. Shaker and H.H. Abdel-Rahman, *Am. J. Appl. Sci.*, 4 (2007) 554–564
 32. M.S. Masoud, A.E. Ali, M.A. Shaker and M.A. Abdul Ghani, *Spectrochim. Acta A.*, 60 (2004) 3155-3159.
 33. E. Cancès, B. Mennucci and J. Tomasi, *J. Chem. Phys.*, 107 (1997) 3032-3042.
 34. R.G. Pearson, *Inorg. Chem.*, 27 (1988) 734-740.
 35. M. Bouklah, N. Benchat, A. Aouniti, B. Hammouti, M. Benkaddour, M. Lagrenee, H. Vezin and F. Bentiss, *Prog. Org. Coat.*, 51 (2004) 118-124
 36. Y. Yan, W. Li, L. Cai and B. Hou, *Electrochim. Acta.*, 53 (2008) 5953-5960
 37. E.S. Feerreira, C. Giancomelli, F. C. Giacomelli and A. Spinelli, *Mater. Chem. Phys.*, 83 (2004) 129–134.
 38. S. S. Abd El-Rehim, M.A.M. Ibrahim and K.F. Khaled, *Mater. Chem. Phys.*, 70 (2001) 268-273
 39. W. Li, Q. He, S. Zhang, C. Pei and B.Hou, *J. Appl. Electrochem.*, 38 (2008) 289.
 40. A. Zarrouk, H. Zarrok, R. Salghi, B. Hammouti, F. Bentiss, R. Tourir and M. Bouachrine., *J. Mater. Environ. Sci.*, 4 (2) (2013) 177-192.
 41. S. Deng, X. Li and H. Fu, *Corros. Sci.*, 53.11 (2011): 3596-3602.
 42. E. E. Oguzie, Y. Li, F. H. Wang, *Journal of colloid and interface science.*, 310(1) (2007) 90-98.
 43. H. Zarrok, R. Saddik, H. Oudda, B. Hammouti, A. El Midaoui, A. Zarrouk, N. Benchat and M. Ebn Touhami, *Der Pharma Chemica.*, 3 (2011) 272-282.
 44. N. Hackerman and E.L. Cook, *J. Electrochem. Soc.*, 97 (1950) 2.
 45. F. Bentiss, M. Traisnel and M. Lagrenee, *Appl. Surf. Sci.*, 161 (2000) 196-202.
 46. N. Hackerman, E.L. Cook, *J. Electrochem. Soc.*, 97 (1) (1950), 1-9.
 47. M. J. Bahrami, S. M. A. Hosseini and P. Pilvar, *Corros. Sci.*, 52 (9) (2010) 2793-2803.
 48. F. Zhang, Y. Tang, Z. Cao, W. Jing, Z. Wu and Y. Chen, *Corros. Sci.*, 61 (2012) 1-9.
 49. M. Galai, M. Rbaa, Y. El Kacimi, M. Ouakki, N. Dkhirech, R. Tourir, B. Lakhrissi, M. Ebn Touhami, *Anal. Bioanal. Electrochem.*, 9 (2017) 80-101.
 50. D.Q. Zhang, Q.R. Cai, X.M. He, L.X. Gao and G.S. Kim, *Mater. Chem. Phys.*, 114 (2009) 612–617.

51. A. Blaqui re, *J. Phys. Radium.*, 13 (1952) 527-540.
52. S. Deng, X. Li and H. Fu, *Corros. Sci.*, 53 (2011) 3596-3602.
53. O. Benali, L. Larabi, M. Traisnel, L. Gengenbre and Y. Harek, *Appl. Surf. Sci.*, 253 (2007) 6130-6139.
54. M. Lebrini, M. Lagren e, H. Vezin, M. Traisnel and F. Bentiss, *Corros. Sci.*, 49 (2007) 2254-2269.
55. X. Wu, H. Ma, S. Chen, Z. Xu and A. Sui, *J. Electrochem. Soc.*, 148 (1999) 208-216.
56. O. Benali., L. Larabi, S.M. Mekelleche, Y. Harek, *J. Mater. Sci.*, 41 (2006) 7064-7073.
57. X.L. Cheng, H.Y. Ma, S. H. Chen, R. Yu, X. Chen and Z.M. Yao, *Corros. Sci.*, 41 (1998) 321-333.
58. M. A. Quraishi, M. W. Khan, M. Ajmal, S. Muralidharan and S. V. Iyer, *Brit. Corros. J.*, 32 (1997) 72-76.
59. R. Tourir, M. Cenoui, M. El Bakri and M. Ebn Touhami, *Corros. Sci.*, 50 (2008) 1530-1537
60. M. Abdallah , *Corros. Sci.*,44 (2002) 717.
61. D.Ben. Hmamou, R. Salghi, A. Zarrouk, H. Zarrok, B. Hammouti, S.S. Al-Deyab, M. Bouachrine, A. Chakir and M. Zougagh, *Int. J. Electrochem. Sci.*, 7 (2012) 5716 -5733.
62. M. El Faydy, M. Galai, A. El Assyry, R. Tourir, M. Ebn Touhami, B. Benali, B. Lakhrissi, A. Zarrouk, *J. Mater. Environ. Sci.*, 7 (2016) 1406.
63. R. T ouir, N. Dkhireche, M. Ebn. Touhami, M. Sfaira, O. Senhaji, J.J. Robin, B. Boutevin and M. Cherkaoui, *Materials Chemistry and Physics.*122 (2010) 1-9.
64. M.Galai ,M. El Faydy, Y.El Kacimi, K.Dahmani, K. Alaoui, R.Touir,B. Lakhrissi, M. Ebn Touhami , *Portugaliae Electrochimica Acta.*, 35(2017)233-251.
65. I. Ahamad, R. Prasad and M.A. Quraishi, *Corros. Sci.*, 52 (2010) 3033-3041.
66. G.E. Badr, *Corros. Sci.*, 52 (2009) 2529-2536.
67. X. Li, S. Deng and H. Fu, *Corros. Sci.*, 53 (2011) 302-309.
68. A.M. Fekry and M.A. Ameer, *Int. J. Hydrogen Energy.*, 35 (2010) 7641-7651
69. Z. Zhang, S. Chen, Y. Li, S. Li and L. Wang, *Corros. Sci.*, 51 (2009) 291-300
70. K. Dahmani, M. Galai, M. Cherkaoui, A. El hasnaoui and A. El Hessni, *J. Mater. Environ. Sci.*, 8 (2017) 1676.
71. M. Elayyachy, M. Elkodadi, A. Aouniti, A. Ramdani, B. Hammouti, F. Malek and A. Elidrissi, *Mat. Chem. Phys.*, 93 (2005) 281-285.
72. N.M. Guan, L. Xueming and L. Fei, *Mater. Chem. Phys.*, 86 (2004) 59-68.
73. A. Tazouti, M. Galai, R. Tourir, M. Ebn Touhami, A. Zarrouk, Y. Ramli, M. Sara o lu, S. Kaya, F. Kandemirli and C. Kaya, *J.Mol.Liq.*, 221 (2016) 815-832
74. E.A. Noor, *Int. J. Electrochem. Sci.*, 2 (2007) 996-1017.
75. I. El Ouali, B. Hammouti, A. Aouniti, X. Ramli, Y. Azougagh, E.M. Essassi and M. Bouachrine, *J. Mater. Envir. Sci.*, 1 (2010) 1-8.
76. P. Cardoso, F.A. Reis, F.C. Massapust, J.F. Costa, L.S. Tebaldi, L.F.L. Ara jo, M.V.A. Silva, T.S.Oliveira, J.A.C.P. Gomes, E. Hollauer, *Quim. Nova.*, 28 (2005) 756-760
77. M. Galai, M. El Gouri, O. Dagdag, Y. El Kacimi, A. Elharfi, and M. Ebn Touhami, *J. Mater. Environ. Sci.*, 7 (5) (2016) 1562.
78. M.J. Frisch, G.W. Trucks, H.B. Schlegel, G.E. Scuseria, M.A. Robb, J.R. Cheeseman, J.A. Montgomery, T. Vreven, K.N. Kudin and J.C. Burant, *Gaussian 03, Revision B. Pittsburgh, PA, USA: Gaussian, Inc.*, (2003).
79. P. Zhao, Q. Liang and Y. Li, *Appl. Surf. Sci.*, 252 (2005) 1596-1607.
80. A. Y. Musa, A.B. Mohamad, A.A.H. Kadhum, M.S. Takriff and W. Ahmoda, *J. Indus. Eng. Chem.*, 18 (2012) 551-555.
81. A. Popova and M. Christov, Deligeorigiev, T. *Corros.*, 59 (2003) 756-764.
82. M. Sahin, G. Gece, F. Karci and S. Bilgic, *J. Appl. Electrochem.*, 38 (2008) 809-815.
83. M.A. Quraishi and R. Sardar. *J. Appl. Electrochem.*, 33 (2003) 1163-1168.
84. V.S. Sastri and J. R. Perumareddi, *Corros.*, 53 (1997) 617.

85. I.B. Obot and N.O. Obi-Egbedi, *Corros. Sci.*, 52 (2010) 657-660.
86. Lukovits, E. Kalman and F. Zucchi, *Corros.*, 57 (2001) 3-9.

© 2018 The Authors. Published by ESG (www.electrochemsci.org). This article is an open access article distributed under the terms and conditions of the Creative Commons Attribution license (<http://creativecommons.org/licenses/by/4.0/>).